PERGAMON

Available online at www.sciencedirect.com

SCIENCE DIRECT®

Continental Shelf Research 23 (2003) 1255–1263

CONTINENTAL SHELF RESEARCH

www.elsevier.com/locate/csr

A surface heat flux climatology over a region of the eastern Bering Sea

Ronald K. Reed

NOAA/Pacific Marine Environmental Laboratory, 7600 Sand Point Way NE, Seattle, WA 98115, USA

Received 4 June 2002; accepted 23 June 2003

Abstract

The eastern Bering Sea shelf is a vast area with weak net circulation. As a result, heat exchange with the atmosphere mainly accounts for changes in heat content of the water column. This region also has marked changes in atmospheric and water properties: for example, winds are light in summer but are relatively strong in winter; air temperatures are 10°C or more in summer but are below freezing in winter; and sea surface temperatures vary from ~10°C to 1°C.

A 29 year time series of cloud cover, relative humidity, wind speed, and air temperature was derived from observations made at St. Paul Island (Pribilof Islands) in the eastern Bering Sea. A time series of sea surface temperature near St. Paul Island was also obtained. Cloud cover during 1965–1994 did not undergo significant changes; relative humidity decreased by a barely significant 3%. Mean wind speed during 1965–1979 was 7.2 m s^{-1} compared with 6.5 m s^{-1} during 1980–1994. Air temperature during 1965–1976 was 1.3°C cooler than during 1977–1994. The mean annual sea surface temperature maximum increased from 8.7°C during 1965–1976 to 9.3°C during 1977–1994.

The seasonal cycles of cloud cover, relative humidity, wind speed, air temperature, and sea surface temperature were then derived from these data and used to calculate the mean monthly and the mean annual surface heat fluxes. Insolation was the dominant flux, followed by latent heat, sensible heat, and net longwave radiation. All of these fluxes have marked seasonal variation. There is a net annual imbalance of 20 W m^{-2}, which is not statistically significant. It could, however, be compensated by weak heat advection from the northward moving currents in the area.
Published by Elsevier Ltd.

Keywords: Bering Sea; Heat budget; Air-sea heat exchange; Weak circulation; Interannual changes

1. Introduction

In much of the ocean, the movement of water across thermal gradients produces substantial changes in heat content of the upper ocean. Examples of this process are warming of the equatorial eastern Pacific during El Niño events or the eastward movement of warm Gulf Stream or Kuroshio waters in the mid-latitude North Atlantic and North Pacific, respectively.

There are other regions, however, where net circulation is very weak, and changes in heat content of the water column are determined largely by air–sea energy exchange. Schumacher and Kinder (1983) and Coachman (1986) showed that the eastern Bering Sea shelf had net flow of only a few cm/s. Reed and Stabeno (1996) and Reed (1998) suggested values of 1–4 cm s^{-1}. Tidal

E-mail address: reed@pmel.noaa.gov (R.K. Reed).

0278-4343/$ - see front matter Published by Elsevier Ltd.
doi:10.1016/S0278-4343(03)00128-6

currents near the Pribilof Islands, however, reach speeds of $\sim 20\,cm\,s^{-1}$ (Kowalik, 1999). Finally, wind-induced currents likely exceed $10\,cm\,s^{-1}$ at times.

Reed (1978) found excellent agreement between surface heat exchange and changes in water column heat content there in summer 1976. Finally, Reed and Stabeno (2002) obtained agreement of surface fluxes and heat content changes within 2% at a shelf site during May–July 1996. Thus, except during occasional storms, heat advection should be small.

The heat budget studies cited were of only brief duration, however, and only in late spring-summer when winds are weak and insolation is the dominant heat flux. The present study examines atmospheric and oceanic variables over the eastern Bering Sea shelf for an extended period of time. Both interannual and seasonal variability are investigated. Finally, the mean annual cycle of surface heat flux is derived.

2. Methods

The Bering Sea shelf region has relatively few ship-of-opportunity weather reports. Shipping between North America and Asia through Unimak Pass is often across the southernmost Bering Sea (see Fig. 1). Although numerous fishing vessels ply the eastern Bering Sea shelf, the annual distribution of any weather reports is poor. As a result of these problems, weather observations from St. Paul Island (Pribilof Islands; Fig. 1) have been used.

2.1. St. Paul Island atmospheric data

Weather observations are made at the St. Paul airport at an elevation of 7 m on the southern part of the island; maximum elevation on the island is 180 m (US Coast Pilot 9, 1997). There is relatively little sea ice near St. Paul Island (Brower et al., 1988). Winds are from all directions, but are often from the north and northeast in winter, spring, and fall. They tend to be from the west and south in summer. A weak anticyclonic current system is usually present around St. Paul Island (Stabeno et al., 1999; Fig. 1).

The frequency of weather reports was variable but was generally hourly or three-hourly. Cloud cover data are missing during 1986, but otherwise extend from 1965 through 1994. To provide a consistent data set, other atmospheric data for 1986 were omitted (Fig. 2).

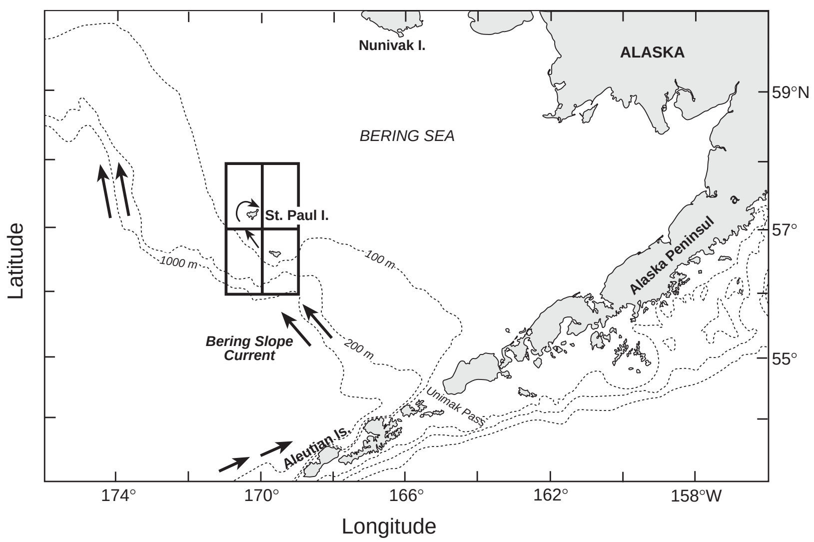

Fig. 1. Location map of the eastern Bering Sea with place names and the 100-, 200-, and 1000-m isobaths. The Bering Slope Current and the anticyclonic shelf flow near St. Paul Island are indicated. The four $1^\circ \times 1^\circ$ areas where data were used are also shown.

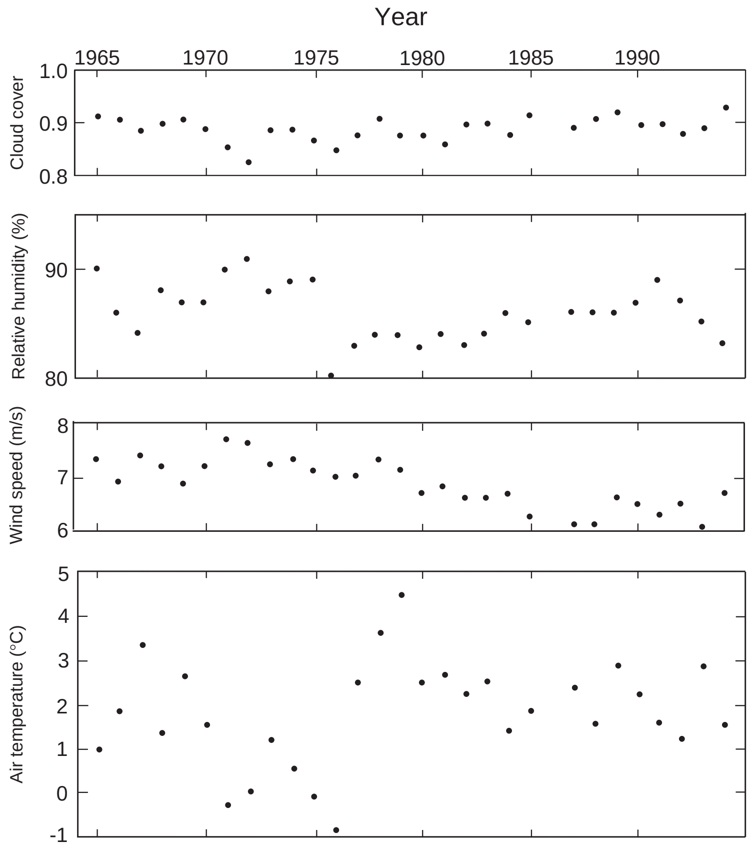

Fig. 2. The annual mean cloud cover, relative humidity (%), wind speed (m s^{-1}), and air temperature (°C) observed at St. Paul Island, 1965–1994.

2.2. Sea surface temperature data

Mean monthly sea surface temperature was derived for each of the four 1° × 1° areas shown in Fig. 1, from 1965 through 1994. Since sea surface temperature was not routinely measured near St. Paul Island, I have used results from the sea surface temperature reanalysis by Kalnay et al. (1996). Bond and Adams (2002) discussed this method in some detail and considered the results to be realistic and useful. The mean sea surface temperature in the region 57–58°N, 169–171°W is ~0.3°C cooler than in the region 56–57°N, 169–171°W. In general, the results used here are in good agreement with those of Brower et al. (1988). It should be noted, however, that Ladd and Bond (2002) found serious errors in derived cloud cover and insolation from the Kalnay et al. (1996) results.

2.3. Heat flux formulas

The exchange of heat across the sea surface may be written as

$$Q_t = Q_s - Q_b - Q_e - Q_h, \quad (1)$$

where Q_t is the total or net exchange, Q_s is the solar radiation (insolation), Q_b is the net back or longwave (infrared) radiation, Q_e is the latent heat flux, and Q_h is the sensible heat flux.

Q_s was derived from the expression

$$Q_s = Q_o(1 - 0.62C + 0.0019\alpha), \quad (2)$$

where Q_o is the insolation under clear skies (from Seckel and Beaudry, 1973), C is cloud cover in tenths, and α is noon solar altitude in degrees. The flux Q_s was reduced by 6% to account for reflected shortwave radiation. Eq. (2), from Reed (1977), has been used often (Weare et al., 1981; Wang and McPhaden, 2001) and has received some independent verification by measurements of insolation at sea (Dobson and Smith, 1988; Reed and Stabeno, 2002).

Q_b, the net longwave radiation, was determined from Efimova's formula (Budyko, 1974)

$$Q_b = \varepsilon\sigma T_s^4(0.254 - 0.00495e_a)(1 - 0.9C) + 4\varepsilon\sigma T_s^3(T_s - T_a), \quad (3)$$

where ε is the emissivity of the sea surface (0.98), σ is the Stefan–Boltzman constant ($5.7\times10^{-8}\,\mathrm{W\,m^{-2}\,K^{-4}}$), e_a is the air vapor pressure in millibars, C is the cloud cover in tenths, and T_s and T_a are absolute sea surface and air temperature, respectively. The cloud factor, 1–0.9C, is that used previously by Reed (1978) for stratus and stratocumulus clouds, which are typical of the Bering Sea. The second term of Eq. (3), involving $T_s - T_a$, is insignificant in the eastern Bering Sea in summer, but is quite important in winter because of cold air temperatures. Eq. (3) was also used by Moisan and Niiler (1998) for the North Pacific south of $\sim$53°N.

Finally, latent and sensible heat fluxes were computed from

$$Q_e = \rho LU(q_s - q_a)C_e, \quad (4)$$

$$Q_h = \rho c_p U(T_s - T_a)C_h, \quad (5)$$

where ρ is the specific air density (1.3×10^{-3}), L is the latent heat of vaporization ($\sim2.5\times10^6\,\mathrm{W\,s\,kg^{-1}}$), U is the wind speed ($\mathrm{m\,s^{-1}}$), c_p is the specific heat capacity of air ($\sim1\times10^6\,\mathrm{W\,s\,m^{-3}\,K^{-1}}$), q_s and q_a are the specific humidity of sea water and air, respectively, T_s and T_a are sea and air temperature near the air–sea interface, and C_e and C_h are exchange coefficients of latent and sensible heat. The values of C_e and C_h were taken as 1.2×10^{-3} and 1.0×10^{-3}, respectively, which are similar to those of Smith (1988), DeCosmo et al. (1996), and earlier results of Friehe and Schmitt (1976) used by Reed (1978). Following results of Esbensen and Reynolds (1981) and Reed and Stabeno (2002), the fluxes were computed from mean monthly properties, rather than from each individual observation. The two methods give results within 10% of each other, and computations from means may be preferable in some instances (Esbensen and Reynolds, 1981).

3. Interannual atmospheric properties

The mean annual cloud cover, relative humidity, wind speed, and air temperature, as observed at St. Paul Island during the period 1965–1994, were determined for each year and are shown in Fig. 2. Hence Fig. 2 shows the interannual variability of properties. Mean annual cloud cover was 0.88 ± 0.02 (standard deviation), with little suggestion of trends. Relative humidity varied between 80% and 91%; the overall mean was $86\pm3\%$. The mean during 1965–1975 was $88\pm2\%$; it was $85\pm2\%$ during 1976–1994. These means are just barely different at the 95% significance level.

Winds at St. Paul Island appear to have been stronger during 1965–1979 than during 1980–1994. During 1965–1979, mean wind speed was $7.2\pm0.2\,\mathrm{m\,s^{-1}}$; during 1980–1994, mean wind speed was $6.5\pm0.3\,\mathrm{m\,s^{-1}}$. Using standard errors, the difference between these means exceeds the 95% significance level. This finding of reduced winds (and decreased latent heat flux) in the latter part of the record is in agreement with findings of Bond and Adams (2001) of recent summer warming of the sea surface. There is also a tendency for weaker winds to be from the south and west, especially in winter–spring (Brower et al., 1988).

The air temperature record shows great year-to-year variability, with the suggestion of a different mean value after 1976 than before. The mean air temperature for the period 1965 through 1976 was 1.0°C, with a standard error (at the 95% significance level) of 1.3°C. During the 1977 through 1994 period, mean air temperature was 2.3°C, with a standard error of 0.9°C. Hence these two means are significantly different. The coldest annual mean (–0.9°C) was in 1976, which also had the greatest percentage of ice cover in the Bering Sea during 1954–1994 (Niebauer et al., 1999). According to Niebauer et al. (1999), and other studies referenced therein, fluctuations in ice cover in the Bering Sea are related to ENSO (El Niño Southern Oscillation) cycles as well as the PDO (Pacific Decadal Oscillation).

Table 1
Interannual variability of cloud cover, relative humidity, wind speed ($m\,s^{-1}$), and air temperature (°C) for each month of the year during 1965–1994. The values given are the mean standard deviations of properties for each month, along with the mean annual values

Month	Cloud cover	Relative humidity (%)	Wind speed ($m\,s^{-1}$)	Air temp. (°C)
January	0.06	4	1.0	2.3
February	0.09	4	1.0	3.8
March	0.09	5	1.0	3.1
April	0.05	5	0.9	2.3
May	0.05	4	0.6	1.6
June	0.04	3	0.7	1.3
July	0.03	2	0.7	1.0
August	0.03	3	0.7	0.9
September	0.04	4	0.6	0.9
October	0.06	4	0.9	1.0
November	0.04	4	1.1	1.5
December	0.04	4	1.2	1.5
Mean annual value	0.05±0.02	4±1	0.9±0.2	1.8±0.9

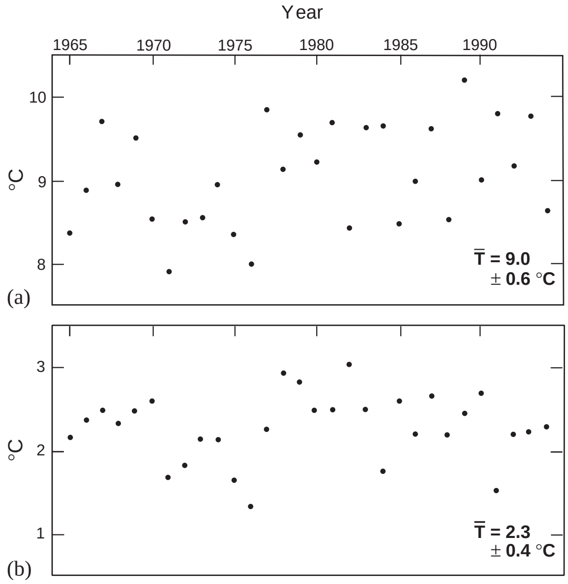

Fig. 3. The mean summer maximum (a) and winter minimum (b) sea surface temperature (°C) averaged over the four 1° × 1° areas shown in Fig. 1, 1965–1994.

Table 1 shows the interannual variability of cloud cover, relative humidity, wind speed, and air temperature for each month of the year. Cloud cover variations were greatest (0.09) in February–March and were least (0.03) in July–August. Variations in relative humidity were largest (5%) in March–April and were smallest (2%) in July. Wind speed variations were largest ($1.2\,m\,s^{-1}$) in December and smallest ($0.6\,m\,s^{-1}$) in May and September. Finally, air temperature variations were greatest (3.8°C) in February and least (0.9°C) in August–September. There is thus a tendency for the largest interannual changes in atmospheric properties to occur in winter and the smallest to occur in summer.

4. Interannual water properties

The sea surface temperature data set (Kalnay et al., 1996) was used to derive the maximum and minimum temperatures each year during 1965–1994. The values used are monthly averages for the four 1° × 1° areas shown in Fig. 1. The annual maximum and minimum values are shown in Fig. 3. The mean maximum temperatures were generally in August and only differ by 0.1°C on average over the four areas. The mean minimum temperatures in March or April, however, differ by 0.5°C, with the two northern areas having a mean minimum of 2.0°C and the two southern areas having a mean minimum of 2.5°C. The coldest sea surface temperature observed, in the northeastern area shown in Fig. 1, was 0.9°C in April 1976, but the area-averaged minimum then was 1.3°C (Fig. 3). The mean sea surface temperature maxima (Fig. 3) are 8.7 (±0.5)°C for 1965–1976 and 9.3(±0.5)°C for 1977–1994. This difference is barely significant at the 95% level. The temperature minima (Fig. 3) for these periods, however, are not significantly different during the two periods above. The interannual variability of sea surface temperature only varies between 0.3°C and 0.6°C and is thus generally smaller than the variability shown in Table 1.

It should be noted that the sea surface isotherms typically extend nearly eastward from the Pribilof Islands to near 165°W (see Fig. 1; Brower et al., 1988). This is a total distance of ~300 km. Thus derived surface heat fluxes (see below) should be, at least approximately, applicable over a substantial area of the shelf. In summary, heating during summer occurs rather uniformly over all four $1^\circ \times 1^\circ$ areas. Also, some winter cooling results from advection of sea ice, especially in the two northern areas, rather than just from direct air–sea heat flux (Stabeno et al., 1999).

5. Seasonal cycles of properties

The mean seasonal cycles of cloud cover, relative humidity, wind speed, air temperature, and sea surface temperature are shown in Fig. 4. Cloud cover has a somewhat complex seasonal distribution. A maximum of 0.96 occurs in July, but a secondary maximum of 0.88 is present in December. Minima (of 0.81) are present in February and March, and a secondary minimum (of 0.84) occurs in October. Relative humidity has maxima of 93% in July–August and a minimum of 81% in November. The period January–April has nearly constant relative humidity. Wind speed has a maximum (of $8.4\,m\,s^{-1}$) in February and a minimum (of $5.0\,m\,s^{-1}$) in July. Although storms may occur at anytime, they are less common

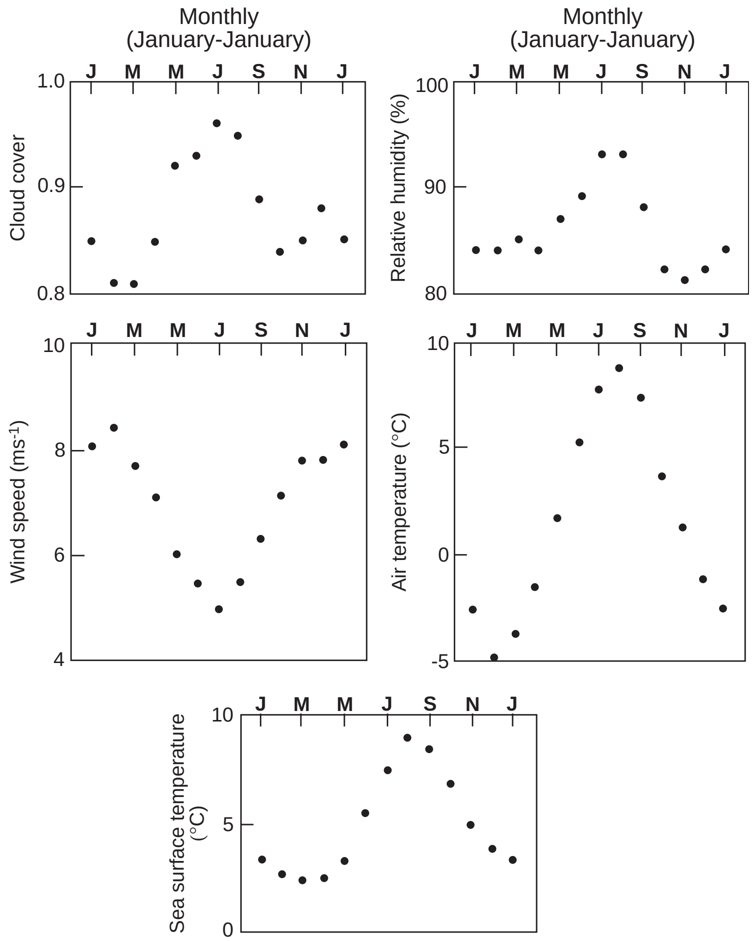

Fig. 4. The mean seasonal variation of cloud cover, relative humidity (%), wind speed ($m\,s^{-1}$), air temperature (°C), and sea surface temperature (°C) during 1965–1994, as discussed in the text.

during May–September than in other months. It should be noted also that winter–spring winds tend to be from the north and east, but summer-fall winds are more typically from all directions (Brower et al., 1988).

Air temperature varies greatly through the year. The minimum (–4.9°C) is in February, and the maximum (8.8°C) is in August. Hence, the seasonal range is nearly 14°C. Sea surface temperature has a minimum in March (2.3°C) and a maximum in August (9.0°C). The seasonal range is thus only about half that of air temperature. This difference mainly occurs because the specific heat of water is four times that of air (McLellan, 1965).

6. Surface heat fluxes

The mean monthly and annual heat fluxes were computed from the 29 year data set as outlined in Section 2c. The results are given in Table 2. Insolation (Q_s) ranges from a high of 172 W m^{-2} in June to a low of 8 W m^{-2} in December. Net longwave radiation (Q_b) varies from a minimum of 8 W m^{-2} in July to a maximum of 55 W m^{-2} in February. The winter values are larger than those in summer because cloud cover is less in winter than summer, air vapor pressure is less in winter than summer, because of cold, dry air, and the sea–air temperature difference is greater in winter than summer (see Eq. (3) and Fig. 4). Latent heat flux is greatest in February (Table 2). This results from relatively strong winter winds and cold, dry air then. Sensible heat flux is also quite large in winter, with values >60 W m^{-2} in January–March, because of strong winds and large sea-air temperature differences then. Except in June and August, the ratios of sensible to latent heat flux (Table 2) are much larger than the typical oceanic values of <0.2 (McLellan, 1965).

The maximum and minimum total heat fluxes (Q_t, Table 2) are in July and February, respectively, and are thus each 1 month prior to the maximum and minimum sea surface temperatures (Fig. 4). The change of sea surface temperature with time (∂SST/∂t; from Fig. 4) has a maximum (increasing with time) between May and June and a minimum (decreasing with time) between October and November. The actual maximum and minimum surface temperatures, however, are in August and March. Thus heating of the sea

Table 2
Mean monthly and annual heat fluxes over the region 56–58°N, 169–171°W for the period 1965–1994

Month	Q_s (Insolation)	Q_b (Net longwave radiation)	Q_e (Latent heat flux)	Q_h (Sensible heat flux)	Q_t (Total heat flux)
January	13	45	64	61	–157
February	34	55	72	82	–175
March	71	49	58	62	–98
April	116	36	44	37	–1
May	150	19	22	12	97
June	172	12	12	1	147
July	158	8	4	–2	148
August	125	11	10	1	103
September	86	15	30	11	30
October	47	34	55	30	–72
November	19	36	60	39	–116
December	8	39	63	51	–145
Means (±std. dev.)	83±60	30±16	41±24	32±28	–20±122
s.e. (95%)	35	9	14	16	71

The fluxes are in units of W m^{-2}. The total heat flux, $Q_t = Q_s – Q_b – Q_e – Q_h$. The standard deviations, and standard errors (s.e.) at 95% significance are also given with the mean fluxes.

surface is a more rapid process than its subsequent cooling, which requires mixing as a result of increasing winds in fall (see Fig. 4).

It is of interest to compare the fluxes derived here with those from brief periods in summer 1976 (Reed, 1978) and May–July 1996 (Reed and Stabeno, 2002). During June–early August 1976, the flux derived was 139 W m^{-2} versus the comparable climatological value from the data here of 141 W m^{-2}. During May–July 1996, the value obtained was 142 W m^{-2} versus the climatological value (Table 2) of 131 W m^{-2}. Bond and Adams (2002) found a correlation between summer 1996 data (Reed and Stabeno, 2002) and results from the reanalysis product (Kalnay et al., 1996) of 0.70. These comparisons suggest that results from a few months duration can give meaningful and useful results.

The total or net heat flux (Q_t) is positive and large during May–August and strongly negative during October–March (Table 2). Its standard deviation (122 W m^{-2}) is much larger than those for any individual component. The mean total or net heat flux is –20 W m^{-2} or 11% of the absolute magnitude of the sum of the four mean surface fluxes. This net heat loss would imply a cooling of the upper ocean over a decadal time scale. This is counterintuitive, however. For example, the results here, as well as those presented by Niebauer et al. (1999), suggest warming in the Bering Sea since the late 1970s. Considering the large standard deviations in the flux terms (Table 2), it may be that the –20 W m^{-2} total flux is not real. A heat loss in this area though could be compensated by heat advection in the relatively warm, northward moving Bering Slope Current (Kinder et al., 1975; see Fig. 1). In addition, Stabeno et al. (1999) presented evidence for an anticyclonic shelf flow around St. Paul Island, which should also result in heat advection there. There are inadequate data on thermal gradients or current speeds, offshore or inshore, to make meaningful estimates of heat advection, however.

A reviewer suggested using the flux fields from the Kalnay et al. (1996) reanalysis to extend the areal coverage beyond the Pribilof Islands region (Fig. 1) that was used here. This would be a dubious undertaking, however. Ladd and Bond (2002) showed that the Kalnay et al. (1996) shortwave radiation, ~350 km east of the Pribilof Islands (at our Mooring 2 which had measured insolation), was overestimated by 70–80 W m^{-2}, presumably as a result of an underestimation of cloud cover. All of the atmospheric variables used here were observed at St. Paul Island (Fig. 1), and only sea surface temperature from the reanalysis, near the Pribilof Islands, was used.

7. Summary

A 29 year time series of weather observations at St. Paul Island, on the eastern Bering Sea shelf, was used to examine the interannual and seasonal structure of atmospheric variables (cloud cover, relative humidity, wind speed, and air temperature). Sea surface temperature for a $2^\circ \times 2^\circ$ area, centered near St. Paul Island, was derived from a recent reanalysis project. These data were used to derive the interannual and seasonal variability of sea surface temperature.

The results here indicate that since the late 1970s, winds are lighter, air temperatures are warmer, and summer maximum, but not winter minimum, sea surface temperatures are warmer. The coldest sea surface temperatures were in 1976, a year of substantial ice cover.

Finally, surface heat fluxes for this 29 year period were derived. In the mean, insolation, latent heat flux, sensible heat flux, and net longwave radiation were, in order, the largest fluxes. These vary greatly by season, however. There is a net annual flux of –20 W m^{-2}, which is not statistically significant. It could, however, be balanced by heat advection from the near-surface circulation.

Acknowledgements

David Kachel obtained the data and prepared them in a useable format. I appreciate the assistance of, and discussions with, Nick Bond and Carol Ladd. Phyllis Stabeno provided support and advice. Comments by a reviewer were quite helpful. This is contribution B413 to the Fisheries

Oceanography Coordinated Investigations and is part of the Coastal Ocean Program of NOAA. Contribution No. 2335 from NOAA/PMEL.

References

Bond, N.A., Adams, J.M., 2002. Atmospheric forcing of the southeast Bering Sea shelf during 1995–99 in the context of a 40 year historical record. Deep-Sea Research II 49, 5869–5887.

Brower Jr., W.A., Baldwin, R.G., Williams Jr., C.N., Wise, J.L., Leslie, L.D., 1988. Climatic Atlas of the Outer Continental Shelf Waters and Coastal Regions of Alaska, Vol. II, Bering Sea. NAVAIR 50-1C-552, MMS87-0012. National Climatic Data Center, NOAA, Asheville, North Carolina and Arctic Environmental Information and Data Center, Univ. Alaska, Anchorage, 519pp.

Budyko, M.I., 1974. Climate and Life. Academic Press, New York, 508pp.

Coachman, L.K., 1986. Circulation, water masses, and fluxes on the southern Bering Sea shelf. Continental Shelf Research 5, 23–108.

DeCosmo, J., Katsaros, K.B., Smith, S.D., Anderson, R.J., Oost, W.A., Bumke, K., Chadwick, H., 1996. Air–sea exchange of water vapor and sensible heat: the humidity exchange over the sea (HEXOS) results. Journal of Geophysical Research 101, 12001–12016.

Dobson, F.W., Smith, S.D., 1988. Bulk models of solar radiation at sea. Quarterly Journal of the Royal Meteorological Society 114, 165–182.

Esbensen, S.K., Reynolds, R.W., 1981. Estimating monthly averaged air–sea transfers of heat and momentum using the bulk aerodynamic method. Journal of Physical Oceanography 11, 457–465.

Friehe, C.A., Schmitt, K.F., 1976. Parameterization of air–sea interface fluxes of sensible heat and moisture by the bulk aerodynamic formulas. Journal of Physical Oceanography 6, 801–809.

Kalnay, E., et al., 1996. The NCEP-NCAR 40-year reanalysis project. Bulletin of the American Meteorological Society 77, 437–471.

Kinder, T.H., Coachman, L.K., Galt, J.A., 1975. The Bering Slope Current system. Journal of Physical Oceanography 5, 231–244.

Kowalik, Z., 1999. Bering Sea tides. In: Loughlin, T.R., Ohtani, K. (Eds.), Dynamics of the Bering Sea. University of Alaska Sea Grant, Fairbanks, Alaska, pp. 93–127.

Ladd, C., Bond, N.A., 2002. Evaluation of the NCEP/NCAR reanalysis in the NE Pacific and the Bering Sea. Journal of Geophysical Research 107 (22), 1–9.

McLellan, H.J., 1965. Elements of Physical Oceanography. Pergamon Press, Oxford, 151pp.

Moisan, J.R., Niiler, P.P., 1998. The seasonal heat budget of the North Pacific: net heat flux and heat storage rates (1950–1990). Journal of Physical Oceanography 28, 401–421.

Niebauer, H.J., Bond, N.A., Yakunin, L.P., Plotnikov, V.V., 1999. An update of the climatology and sea ice of the Bering Sea. In: Loughlin, T.R., Ohtani, K. (Eds.), Dynamics of the Bering Sea. University of Alaska Sea Grant, Fairbanks, Alaska, pp. 29–59.

Reed, R.K., 1977. On estimating insolation over the ocean. Journal of Physical Oceanography 7, 482–485.

Reed, R.K., 1978. The heat budget of a region in the eastern Bering Sea, summer 1976. Journal of Geophysical Research 81, 3635–3645.

Reed, R.K., 1998. Confirmation of a convoluted flow over the southeastern Bering Sea shelf. Continental Shelf Research 18, 99–103.

Reed, R.K., Stabeno, P.J., 1996. On the climatological mean circulation over the eastern Bering Sea shelf. Continental Shelf Research 16, 1297–1305.

Reed, R.K., Stabeno, P.J., 2002. Surface heat fluxes and subsurface heat content at a site over the southeastern Bering Sea shelf, May–July 1996. Deep–Sea Research II 49, 5911–5917.

Seckel, G.R., Beaudry, F.H., 1973. The radiation from sun and sky over the North Pacific Ocean (abstract). EOS Transactions American Geophysical Union 54, 1114.

Smith, S.D., 1988. Coefficients for the sea surface wind stress, heat flux and wind profiles as a function of wind speed and temperature. Journal of Geophysical Research 93, 15467–15474.

Stabeno, P.J., Schumacher, J.D., Salo, S.A., Hunt Jr., G.L., Flint, M., 1999. Physical environment around the Pribilof Islands. In: Loughlin, T.R., Ohtani, K. (Eds.), Dynamics of the Bering Sea. University of Alaska SeaGrant, Fairbanks, Alaska, pp. 193–215.

US Coast Pilot 9, 1997. Pacific and Arctic Alaska: Cape Spencer to Beaufort Sea. US Department of Commerce, National Oceanic and Atmospheric Administration, National Ocean Service, pp. 306–309.

Wang, W., McPhaden, M.J., 2001. What is the mean seasonal cycle of surface heat flux in the equatorial Pacific? Journal of Geophysical Research 106, 837–857.

Weare, B.C., Strub, P.T., Samuel, M.D., 1981. Annual mean surface heat fluxes in the tropical Pacific. Journal of Physical Oceanography 11, 705–717.